

Organic Thin-Film Transistors with Conductive Metal–Oxides as Source–Drain Electrodes

Musubu ICHIKAWA*, Li YOU, Shuhei TATEMACHI, Toshiki KOYAMA and Yoshio TANIGUCHI

Department of Functional Polymer Science, Faculty of Textile Science and Technology, Shinshu University,
3-15-1 Tokita, Ueda, Nagano 386-8567, Japan

(Received September 20, 2006; accepted October 17, 2006; published online November 2, 2006)

We demonstrated that bottom contact (BC) configuration organic thin-film transistors (OTFTs) easily get higher performance by using conductive metal oxide (CMO) as source and drain electrodes. Although BC-OTFTs are more advantageous than top contact (TC) configuration in the viewpoint of device fabrications, it is also well-known that BC-OTFTs show poor performance compared with TC-OTFTs with the same active material. We found out that using CMO like indium tin oxide as contact electrodes enhanced performance of BC-OTFTs without any special surface treatments. This manner was truly effective for most organic semiconducting materials, for example, pentacene, polythiophene, and so on.

[DOI: 10.1143/JJAP.45.L1171]

KEYWORDS: organic transistor, organic TFT, bottom contact, pentacene, ITO

In recent years organic electronic devices have gained special interest due to their potentials for flexible, large-area, and low-cost electronic applications.^{1,2)} Similar to amorphous silicon field-effect transistors (FETs) organic FETs are commonly fabricated using thin-film transistor (TFT) design concepts. Possible configurations are top contact (TC), where source drain electrodes are evaporated onto the organic film, and bottom contact (BC), where the organic film is deposited on a substrate already patterned with all (source, drain, and gate) electrodes. As generally known the performance of the organic TFTs with BC configuration is inferior to that of the TC configuration TFT with the same active material.³⁾ Consequently, most high-performance organic TFTs reported in the literature have the TC configuration, and shadow masking is generally used to pattern the source and drain contacts on the top of the organic thin-film. Unfortunately, this does not suit for commercial manufacturing. On the other hand, BC configuration is more preferable because this allows conventional fine photolithographic patterning of the source and drain electrodes with no-exposure of the active organic thin-film to solvents and chemicals. Furthermore, BC configuration is also advantageous to accelerate the research on channel materials because this type TFT is easily fabricated with just depositing a channel material onto a ready-made backplane, where a backplane means a substrate with patterned source, drain and gate electrodes and gate dielectrics.

It is generally accepted that the reduction of TFT performance on BC configuration results from poor thin-film growth on and close to “metal” contact electrodes due to large surface energy difference between the electrodes and gate dielectrics.³⁾ The poor growth results in lowering of charge carrier mobility and also causes large electric contact resistance between FET-channel and contact electrodes.^{4–6)} To improve the performance of BC configuration organic TFTs, several approaches such as self-assembled monolayer treatment of the BC backplane surface,^{7,8)} and introducing buffer-layer between the contact electrodes and gate insulator^{6,9)} were proposed. On the contrary to these research steams, there is no report to improve the device performance of BC organic TFTs based on metal species of the BC

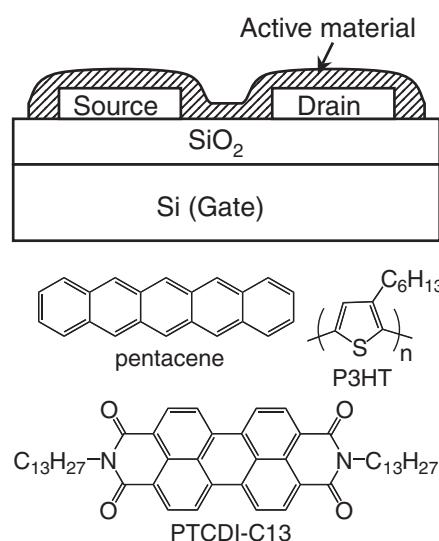


Fig. 1. (a) Schematic device structure of organic TFTs and (b) chemical structures used in this study.

electrode. Kymissis *et al.* pointed out that the different surface energies of the dielectrics and the electrodes led to different morphologies and thus to reduced device performance.⁷⁾ By extension of this discussion, conductive metal oxide (CMO) is a promising candidate as source and drain electrodes of BC configuration organic TFTs because some metal oxides like Ta₂O₅, Al₂O₃, SiO₂, and so on are fully proven gate dielectrics of organic TFTs. In this article, we demonstrate that CMOs like indium tin oxide (ITO) and indium zinc oxide (IZO) improve the device performance of various organic TFTs with BC configuration without any surface treatment of BC backplanes.

Figure 1 shows the device structure of fabricated TFTs. The TFTs were prepared by depositing organic active materials onto a backplane, which consisted of a heavily doped Si wafer with a 400-nm-thick SiO₂ layer (specific capacitance of 7.5 nF/cm²) and pre-formed source and drain electrodes. The Si wafer worked as a gate electrode. The source and drain electrodes were prepared by vacuum deposition of gold through a shadow mask. On the other hand, CMO source and drain electrodes were fabricated as

*Corresponding author. E-mail address: musubu@shinshu-u.ac.jp

follows: (1) 150-nm-thick ITO or IZO layer was deposited onto the Si wafer by sputtering, (2) source and drain electrodes were patterned by conventional photolithography and wet-etching. The backplanes with ITO or IZO source and drain electrodes (abbreviated as ITO or IZO backplane) were washed with organic solvent to degrease the surface before use. Note that after no change of the CMO thickness was confirmed after the etching. Another Au backplane was not treated after depositing source and drain electrodes. The channel length (L) and width (W) were, respectively, about $50\ \mu\text{m}$ and $2\ \text{mm}$. Following organic semiconductors were used as active layers: pentacene, N, N'-ditridecyl-3,4,9,10-perylenetetracarboxylic diimide (PTCDI-C13), and regioregular poly(3-hexylthiophene) (P3HT), whose structures were shown in Fig. 1. Excepting for P3HT, the organic active materials were deposited with thermal evaporation onto backplanes at the rate of $0.3\text{--}0.5\ \text{\AA}/\text{s}$ under a vacuum ($8.0 \times 10^{-4}\ \text{Pa}$), and P3HT was spin-casted onto backplanes from 1-wt % *o*-dichlorobenzene solution. It should be noted here that a material was deposited onto each backplane at the same time to evade performance variations from deposition to deposition. TFT characteristics of devices were measured with an Advantest R6245 2-channel source-measure-unit under a vacuum (below $1 \times 10^{-3}\ \text{Pa}$). X-ray diffraction (XRD) was measured with Cu $K\alpha$ radiation under θ - 2θ geometry. Surface morphologies of thin-films were evaluated with a Seiko SPM-400 atomic force microscope (AFM) with a dynamic force mode. Sample thin-films for XRD and AFM were prepared onto CMO or Au coated substrates that were prepared in the similar manner of the backplanes in the exception of source and drain electrodes patterning.

Figure 2(a) shows source current–drain voltage (I_D - V_D) characteristics at various gate voltages (V_G) of a pentacene TFT with an Au backplane. The TFT, indeed, exhibited poor characteristics. As mentioned before, BC configuration pentacene TFTs without any treatments to improve TFT performances like self-assembling molecular regents generally show poor performances.^{3,6-8,10} On the other hand, as shown in Fig. 2(b), another pentacene TFT with an ITO backplane fabricated at the same time in the above TFT shows excellent I_D - V_D characteristics in p-type operation: linear increasing of I_D in low V_D region and obvious saturation behavior of I_D at high V_D region. I_D of the ITO backplane TFT was much larger than that of the Au backplane TFT. The field-effect hole mobility and the threshold voltage of the ITO backplane TFT were $0.18\ \text{cm}^2/(\text{V}\cdot\text{s})$ and $-28\ \text{V}$, respectively. Figure 2(c) shows I_D - V_D characteristic of the ITO backplane pentacene TFT, and also shows square roots of I_D vs V_G characteristic of the TFT together with that of the reference Au backplane TFT. Figure 3(c) clearly confirms the superior transfer characteristic of the ITO backplane TFT in contrast to the Au backplane TFT. These results strongly indicate that using ITO as source and drain electrode for BC configuration pentacene TFTs easily improve device characteristics.

Figures 3(a) and 3(b) show AFM topological images of pentacene thin-films on Au and ITO. While both figures show similar small grains, details are some different each other. For example, the grains on ITO looked like almost similar size (about $150\ \text{nm}$), and were tightly packed. On

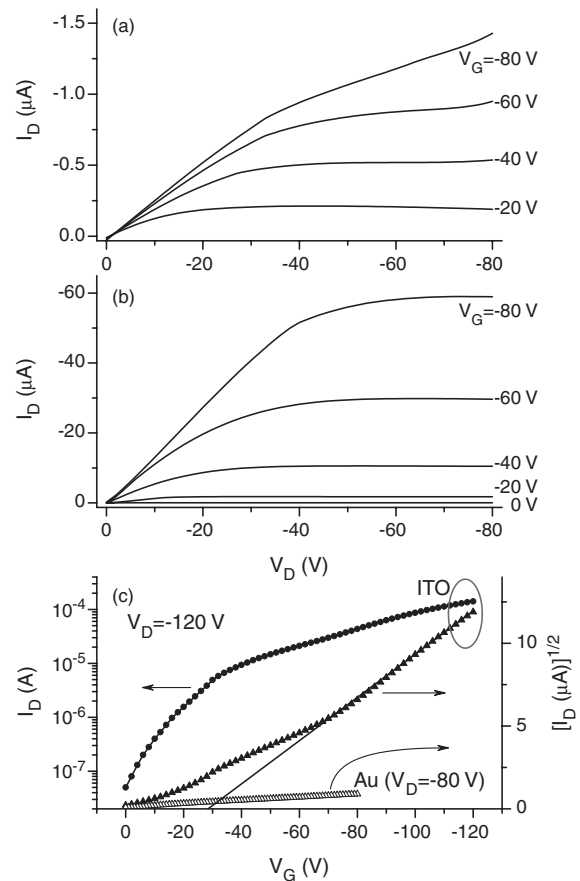


Fig. 2. I_D - V_D characteristics of pentacene TFTs made on Au (a) and ITO (b) backplanes. Each L/W were, respectively, $43\ \mu\text{m}/1.99\ \text{mm}$ and $53\ \mu\text{m}/1.97\ \text{mm}$. (c) I_D - V_G and $I_D^{1/2}$ - V_G characteristics of the pentacene ITO backplane TFT at $V_D = -120\ \text{V}$ with $I_D^{1/2}$ - V_G characteristic of the reference pentacene Au backplane TFT.

the other hand, the grains on Au were showed size variety compared with those on ITO; there were some large agglomerations as observed in Fig. 3(a). In addition, the grains on ITO seem to have clearer edges than those on Au. It is, therefore, supposed that pentacene thin-film on ITO may be more crystalline than that on Au. XRD of each thin-films sufficiently supported the above speculation. As shown in Fig. 3(e), while a pentacene thin-film on Au was definitely amorphous without any reflections except for a broad hollow at around 15° , another thin-film on ITO showed a diffraction peak (but it was weak and broad) at 5.78° that corresponds to d -spacing of $15.3\ \text{\AA}$. This d -spacing was close to that of the thin-film phase of pentacene ($15.4\ \text{\AA}$).¹¹ Note that a reflection at 21.5° was (211) of ITO.¹² However, higher reflections like (002) did not appear in the XRD. We suppose at present that large surface-roughness of polycrystalline ITO film causes the weak and broad diffraction peak. In fact, XRD of pentacene thin-film on IZO, whose surface is much smoother than that of polycrystalline ITO due to its amorphous nature,¹³ exhibited high-order diffraction peaks up to (004) as also shown in the figure. Taking into consideration that bad crystallinity of pentacene thin-film grown on conventional metal BCs causes poor performance of the TFT,³ the formation of the highly oriented pentacene thin-film on CMO contacts probably leads to the higher TFT performance. In addition,

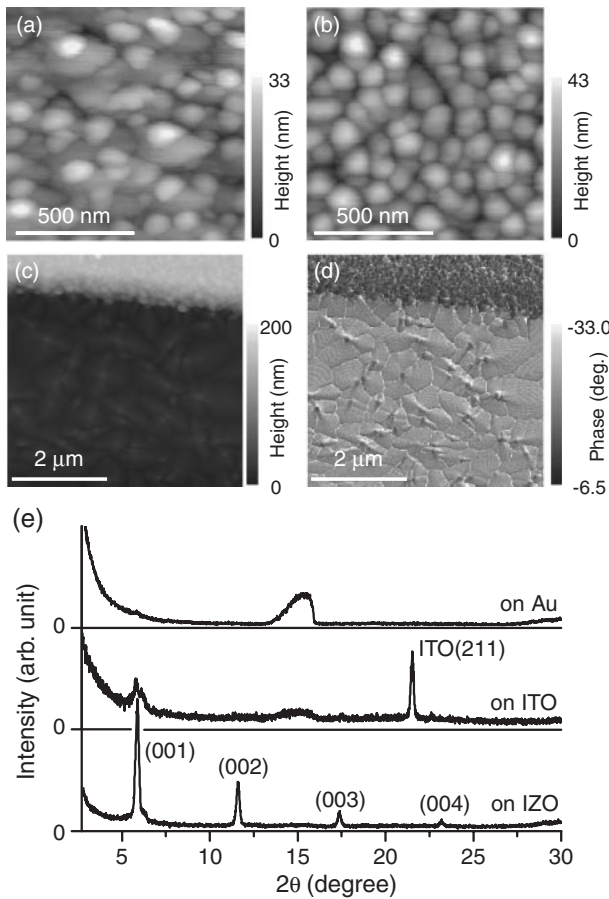


Fig. 3. AFM images of pentacene thin-films on Au (a), ITO (b) and at around the ITO/channel interface (c, d: phase image). (e) XRD patterns of pentacene thin-films on Au, ITO, and IZO.

it is also well-known that the poor performances of Au backplane pentacene TFTs are caused by bad growths of pentacene thin-films at a vicinity region on a TFT channel. Figures 3(c) and 3(d) show AFM topology and phase images of the pentacene thin-film around the ITO/channel interface. Grains of the thin-film on the channel far from the interface grow larger than those on ITO, and the grain size is almost same close by the interface as shown in the phase image [Fig. 3(d)]. The good growth at the vicinity of the interface probably leads to the good performance of the ITO backplane TFT.

Figures 4(a), 4(b), and 4(c) show I_D - V_D characteristics of other organic TFTs with CMO BC electrodes. As clearly shown in the figure, all TFTs exhibited good performance; the pentacene TFT with an IZO backplane also exhibited a good performance with the field-effect mobility of $0.062 \text{ cm}^2/(\text{V}\cdot\text{s})$ and the threshold voltage of -30 V . In addition, the IZO backplane PTCDI-C13 TFT clearly showed an n-type enhancement operation with a threshold voltage of 23.8 V and rather high field-effect mobility of $0.25 \text{ cm}^2/(\text{V}\cdot\text{s})$. To the best of our knowledge, this PTCDI-C13 TFT exhibits the highest field-effect electron mobility as a BC type organic TFT. On the other hand, another BC configuration PTDI-C13 TFT with an Au backplane did not work. Moreover, the bottom configuration P3HT TFT with an ITO backplane exhibited better performance compared with another BC type P3HT TFT with an Au backplane;

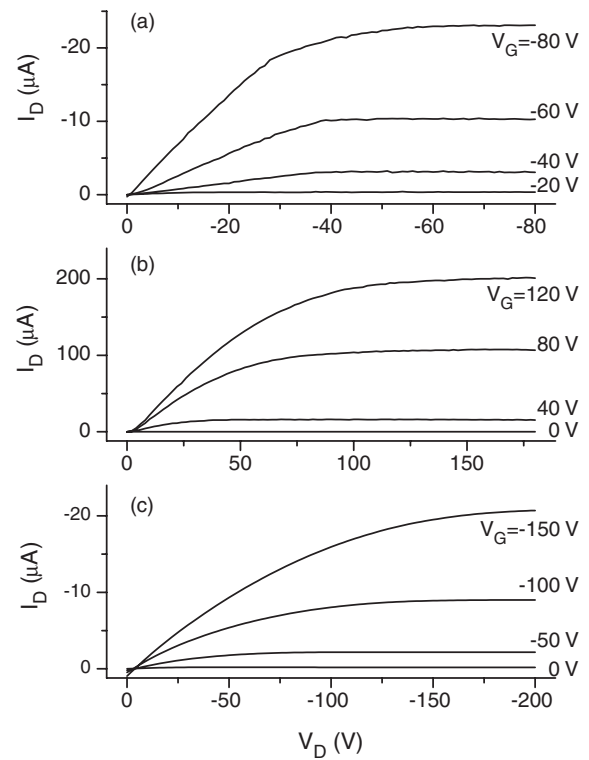


Fig. 4. I_D - V_D characteristics of (a) pentacene TFT on IZO backplane, (b) PTCDI-C13 TFT on IZO backplane, (c) P3HT TFT on ITO backplane. Each L/W were, respectively, $49.5 \mu\text{m}/1.75 \text{ mm}$, $45.7 \mu\text{m}/1.96 \text{ mm}$, and $50 \mu\text{m}/1.94 \text{ mm}$.

while the Au backplane P3HT TFT showed normally-ON behavior (threshold voltage was $+44 \text{ V}$), that with the ITO backplane exhibited normally-OFF characteristic (threshold voltage was -32 V). In addition, field-effect hole mobility of the ITO backplane P3HT TFT [$0.012 \text{ cm}^2/(\text{V}\cdot\text{s})$] was much higher than that of the Au backplane TFT [$1.0 \times 10^{-3} \text{ cm}^2/(\text{V}\cdot\text{s})$]. These results fully prove that CMOs suit for source and drain electrodes for almost all organic TFTs with BC configuration. While enhancements of mobility probably cause good thin-film growth properties on and close to CMOs as mentioned above, we scarcely understand at present the reason why CMO backplanes provide normally-OFF characteristic to organic TFTs. However, the normally off behavior is important for switching and logic circuits.

In conclusion, we demonstrated that the performance of pentacene TFTs with BC configuration improved without any special surface treatments when CMOs were used as source and drain electrodes. We also showed that this manner was effective to various kind of organic semiconductor including n-type materials and polymer materials. Combination of the CMO backplanes and proven surface treatment techniques probably brings high performance BC configuration organic TFTs whose performances are comparable to that of TC configuration organic TFTs into reality.

This work was supported by the Cooperative Link for Unique Science and Technology for Economy Revitalization (CLUSTER) of the Ministry of Education, Culture, Sports, Science and Technology, Japan. It was also supported by the Ministry's 21st Century Center of Excellence (COE) program.

- 1) C. D. Dimitrakopoulos and P. R. L. Malenfant: *Adv. Mater.* **14** (2002) 99.
- 2) G. Horowitz: *Adv. Mater.* **10** (1998) 365.
- 3) C. D. Dimitrakopoulos and D. J. Maseo: *IBM J. Res. Dev.* **45** (2001) 11.
- 4) L. Bürgi, T. J. Richards, R. H. Friend and H. Sirringhaus: *J. Appl. Phys.* **94** (2003) 6129.
- 5) J. A. Nichols, D. J. Gundlach and T. N. Jackson: *Appl. Phys. Lett.* **83** (2003) 2366.
- 6) N. Yoneya, M. Noda, N. Hirai, K. Nomoto, M. Wada and J. Kasahara: *Appl. Phys. Lett.* **85** (2004) 4663.
- 7) I. Kyriakidis, C. D. Dimitrakopoulos and S. Purushothaman: *IEEE Trans. Electron Devices* **48** (2001) 1060.
- 8) C.-K. Song, B.-W. Koo, S.-B. Lee and D.-H. Kim: *Jpn. J. Appl. Phys.* **41** (2002) 2730.
- 9) T. Muck, J. Fritz and V. Wagner: *Appl. Phys. Lett.* **86** (2005) 232101.
- 10) A. Salleo, M. L. Chabinyc, M. S. Yang and R. A. Street: *Appl. Phys. Lett.* **81** (2002) 4383.
- 11) C. D. Dimitrakopoulos, A. R. Brown and A. Pomp: *J. Appl. Phys.* **80** (1996) 2501.
- 12) C. Liu, T. Matsutani, T. Asanuma, K. Murai, M. Kiuchi, E. Alves and M. Reis: *J. Appl. Phys.* **93** (2003) 2262.
- 13) T. Sasabayashi, N. Ito, E. Nishimura, M. Kon, P. K. Song, K. Utsumi, A. Kaijo and Y. Shigesato: *Thin Solid Films* **445** (2003) 219.